LASER
& PHOTONICS
REVIEWS

Laser Photonics Rev. **8,** No. 5, 750–755 (2014) / **DOI** 10.1002/lpor.201400017

ORIGINAL PAPER

Abstract The discovery of a novel phase-locked frequency comb generated from a monolithic laser with the concurrent processes of self-mode locking (SML) and stimulated Raman scattering (SRS) is reported. It is experimentally shown that the width of the Raman gain can be exploited to considerably expand the frequency comb of a monolithic SML crystal laser via the SRS process. At a pump power of 6.5 W, an output power of 140 mW in the Stokes wave with a pulse width as narrow as 2.9 ps at a pulse repetition rate of 6.615 GHz is obtained. The present finding not only provides useful insights into the monolithic intracavity SRS process but also paves the way for generating mode-locked pulses based on monolithic self-Raman crystals.

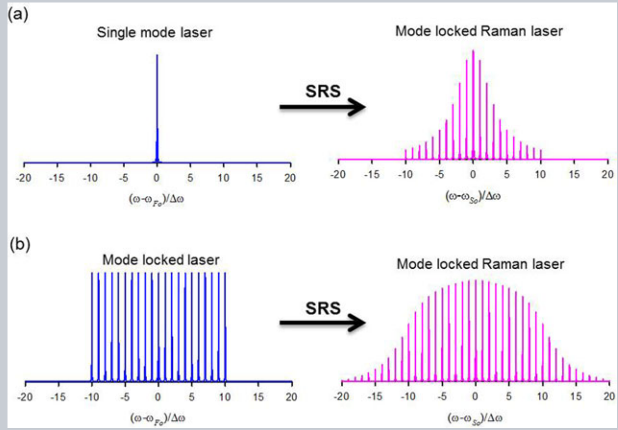

Frequency comb expansion in a monolithic self-mode-locked laser concurrent with stimulated Raman scattering

C. Y. Lee[1], C. C. Chang[1], H. C. Liang[2], and Y. F. Chen[1,3,*]

1. Introduction

Development of laser sources with picosecond and femtosecond durations has led to a significant revolution on molecular spectroscopy, condensed-matter physics, nonlinear optics, frequency metrology, telecommunications, and biomedical sensing [1–4]. The approaches for generating such high repetition rate pulses include the four-wave mixing in microresonators [5–8] and the mode locking in solid-state lasers [9,10] or semiconductor-based systems [11,12]. Thanks to the development of diode-pumping techniques, it has been found that the mode locking can be self-achieved in Yb:KY$(WO_4)_2$ [13], Yb:KGd$(WO_4)_2$ [14], Yb:YVO_4 [15], Yb:Y_2O_3 [16], Yb:YAG [17], Nd:YVO_4 [18,19], and Nd:$GdVO_4$ [20] crystal lasers. This kind of mode locking without using active or passive mode-locking elements (such as saturable absorbers) except for the gain medium is generally called self-mode locking (SML). The origin of the SML so far is proposed to be associated with the combined effect of the Kerr lensing and thermal lensing [13–18].

One intriguing feature is that the laser crystals used to achieve the SML operation naturally possess several intense isolated Raman bands in the spontaneous Raman spectra. This characteristic enables the laser crystal for achieving the SML to also be excellent Raman gain media for performing wavelength conversion via stimulated Raman scattering (SRS) [21–25]. Similar to the Kerr effect, the SRS is a nonlinear optical process to be also associated with the third-order $\chi^{(3)}$ nonlinearity. Recently, it has been discovered that a Raman frequency comb can be generated with a single-frequency laser to pump a whispering-gallery-mode cavity due to the width of the Raman gain [26]. This discovery provokes an interesting issue whether the SML can be simultaneously achieved in a self-Raman laser to expand the frequency comb via the SRS process.

In this work we successfully demonstrate that a novel phase-locked frequency comb can be generated with a monolithic SML laser concurrent with the SRS process. We show that the longitudinal modes of the Stokes wave generated in a monolithic Nd:YVO_4 laser can be phase locked, and actually be mutually coherent. Just below the SRS threshold, the monolithic laser is found to emit the fundamental wave with a frequency comb of 22 longitudinal modes. Above the SRS threshold, we observe that the monolithic laser predominantly emits the Stokes wave with a Raman frequency comb of 34 longitudinal modes. In the meanwhile, we also find the central longitudinal modes of the fundamental wave to be significantly depleted. At a pump power of 6.5 W, we obtain an output power of 140 mW in the Stokes wave with a pulse width as narrow as 2.9 ps at a pulse repetition rate of 6.615 GHz. The present result not only evidences the feasibility of the frequency comb expansion in a monolithic SML laser

[1] Department of Electrophysics, National Chiao Tung University, 1001 Ta-Hsueh Rd., Hsinchu 30010, Taiwan
[2] Institute of Optoelectronic Science, National Taiwan Ocean University, Keelung 20224, Taiwan
[3] Department of Electronics Engineering, National Chiao Tung University, 1001 Ta-Hsueh Rd., Hsinchu 30010, Taiwan
*Corresponding author: e-mail: yfchen@cc.nctu.edu.tw

concurrent with SRS but also paves the way for the development of a new class of mode-locked lasers based on monolithic self-Raman crystals.

2. Principles

The linewidth broadening of Raman transitions in crystals is generally homogeneous and can be described with a Lorentzian profile. The stimulated Raman gain profile for a Raman crystal pumped by a fundamental wave with a narrow laser line ω_F is then given by [27]

$$g_R(\omega) = \frac{8\pi c^2 N_o}{\hbar n_s^2 \omega^3 \Gamma}\left(\frac{\partial\sigma}{\partial\Omega}\right)\frac{\Gamma}{(\omega-\omega_S)^2+\Gamma^2}, \quad (1)$$

where $\omega_S = \omega_F - \omega_R$ is the central frequency of the Stokes wave, ω_R is the frequency of the Raman shift, Γ is the linewidth of the Raman transition (half-width at half-maximum), $\partial\sigma/\partial\Omega$ is the integrated scattering cross section, N_o is the number of Raman-active molecules, and n_s is the refractive index of the Raman media for the Stokes frequency. Provided that the lasing modes of the Stokes waves are phase locked in a high-Q resonator, the frequency distribution for the Raman comb can be expressed as

$$\begin{aligned} I_S(\omega) &= \sum_{m=-M}^{M}\frac{\Gamma}{(\omega-\omega_S)^2+\Gamma^2}\delta(\omega-\omega_S-m\Delta\omega) \\ &= \sum_{m=-M}^{M}\frac{\Gamma}{(m\Delta\omega)^2+\Gamma^2}\delta(\omega-\omega_S-m\Delta\omega), \quad (2) \end{aligned}$$

where $\Delta\omega$ is the frequency spacing of the cavity mode and the effective number of the Raman comb is $2M+1$. Based on the Lorentzian distribution, the number M can be approximately determined by the integer closest to the value of $2\Gamma/\Delta\omega$. In other words, the number of the cavity modes inside a Raman comb mainly depends on the gain width Γ and the mode spacing $\Delta\omega$. To explicitly present the frequency distribution, the δ-function in Eq. (2) is replaced with an analytical function derived from the damped harmonic oscillator, i.e.

$$I_S(\omega) = \frac{2}{\pi}\sum_{m=-M}^{M}\frac{\Gamma}{(m\Delta\omega)^2+\Gamma^2}\frac{\gamma\omega^2}{[\omega^2-(\omega_S+m\Delta\omega)^2]^2+(\gamma\omega)^2}, \quad (3)$$

where γ is the effective linewidth of the fundamental wave. Provided that a laser crystal can be used to simultaneously achieve SML and SRS, the central Stokes frequency ω_S can be expanded to be multiple components of $\omega_S = \omega_{So} + n\Delta\omega$ with the integer n ranging from $-N$ to N, where the number of lasing modes in the fundamental wave is assumed to be $2N+1$. Consequently, the frequency distribution for the Raman comb generated with SML fundamental wave can be given by

$$I_S(\omega) = \frac{2}{\pi}\sum_{m=-M}^{M}\sum_{n=-N}^{N} \times\frac{\Gamma}{(m\Delta\omega)^2+\Gamma^2}\frac{\gamma\omega^2}{[\omega^2-(\omega_{So}+(n+m)\Delta\omega)^2]^2+(\gamma\omega)^2}. \quad (4)$$

Figures 1a and b illustrate the example of the Raman comb generated with a single-frequency and a mode-locked fundamental wave, respectively. The values of the parameters are given by: $\Delta\omega = 6.6$ GHz, $\Gamma = 20$ GHz,

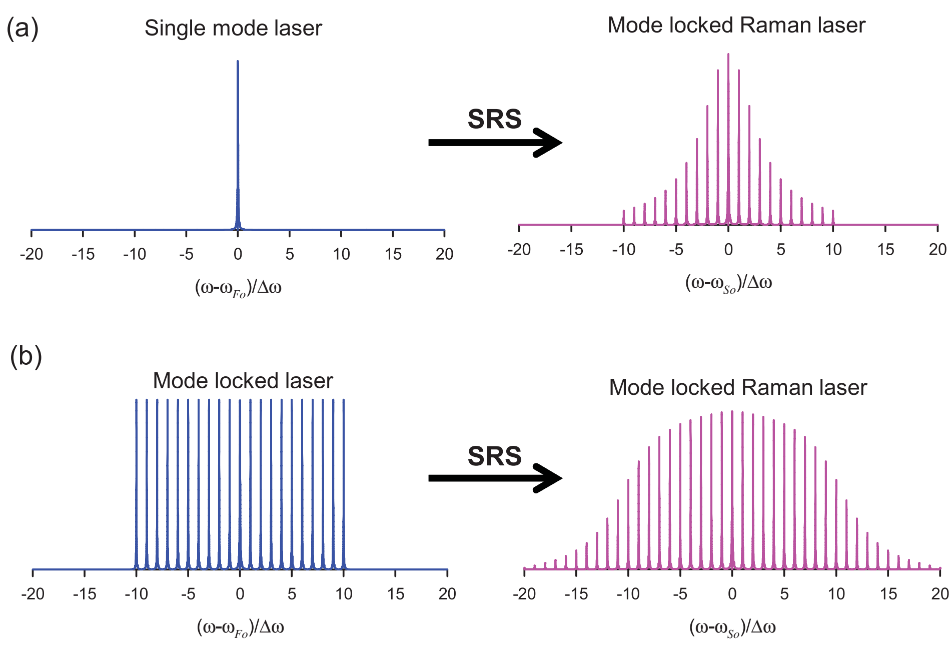

Figure 1 Illustration for the Raman frequency comb generated with (a) a single-frequency and (b) a mode-locked fundamental wave, respectively.

$\gamma = 10$ kHz, and $N = 0$ for the single-frequency source and $N = 10$ for the mode-locked source.

3. Experimental results and discussion

For realizing the simultaneous SRS and SML, we first exploited a single gain medium with dielectric coatings to form a monolithic high-Q Fabry–Perot resonator. Figure 2 shows the experimental setup for the monolithic laser cavity with SML and SRS operation concurrently. The gain medium was an *a*-cut 0.3 at.% doped Nd:YVO_4 crystal with a length of 8 mm. The front end of the gain medium was diffusion bounded with a 2.5-mm undoped YVO_4 to reduce the thermal effects. As a result, the total length of the laser crystal was approximately 10.5 mm. The front facet of the laser crystal was coated for superhigh reflection at the fundamental wavelength of 1064 nm ($R > 99.99\%$) and the Stokes wavelength of 1176 nm ($R > 99.99\%$) and high transmission at the pump wavelength of 808 nm ($T > 95\%$) to serve as the front mirror. The rear facet was coated for superhigh reflection at 1064 nm ($R > 99.99\%$) and intermediately high reflection at 1176 nm ($R \approx 99.95\%$) to serve as the output coupler for the first Stokes wave. The laser crystal was wrapped with indium foil and mounted within a water-cooled copper heat sink at 10 °C. The pumping source was a 808-nm fiber-coupled laser diode with a core diameter of 200 μm and a numerical aperture of 0.2. A lens with a focal length of 25 mm was used to focus the pump beam into the laser crystal. The overall coupling efficiency was nearly 90%. The pump spot radius was approximately 100 μm.

Figure 3a depicts the average output power versus the incident pump power for the monolithic self-Raman laser. The lasing thresholds are approximately 1.0 W and 3.3 W for the fundamental and Stokes waves, respectively. The average output power of the fundamental wave can be seen to be kept at a level of 45 mW for the pump power beyond the SRS threshold. The clamping of the output power agrees with the theoretical prediction that the intracavity power of the fundamental wave is almost fixed at its value at the SRS threshold for higher pump powers [27]. On the other hand, the average output power of the Stokes wave can be seen to linearly increase on increasing the pump power beyond the SRS threshold. At a pump power of 6.5 W, the average output power of the Stokes wave is approximately 140 mW. The optical spectrum was measured with a Michelson interferometer (Advantest Q8347) with a resolution as high as 0.003 nm to directly observe the mode structure. Figure 3b depicts the optical spectrum for the fundamental wave at a pump power of 3.2 W, i.e. just below the SRS threshold. The optical spectrum can be seen to exhibit 22 lasing modes with the central frequency near 1064.45 nm. Above the SRS threshold, some central longitudinal modes of the fundamental wave are found to be depleted so as to destroy the comb structure, as shown in Fig. 3c for the optical spectrum measured at a pump power of 6.5 W. Figure 3d shows the optical spectrum for the Stokes waves obtained at the same pump power. It can be seen that the optical spectrum for the Stokes wave displays a coherent self-Raman frequency comb with the number of lasing modes up to 34. The mode spacing is approximately 0.025 nm, which is exactly consistent with the free spectral range of the optical cavity length.

An RF spectrum analyzer (Agilent) with a bandwidth of 26.5 GHz was exploited to analyze the temporal behavior of the laser output. The mode-locked pulse was also detected by a high-speed InGaAs photo-detector (Electro-optics Technology, Inc. ET-3500 with rise time of 35 ps) whose output signal was connected to the RF spectrum analyzer. Figure 4 shows the RF spectrum for the Stokes wave with a span of 26.5 GHz and a resolution bandwidth of 100 kHz. The fundamental frequency peak can be seen to be 6.615 GHz, which corresponds exactly to the free spectral range of the optical cavity length. Furthermore, the amplitudes of the signal to noise for the fundamental and second-harmonic peaks are nearly up to 50 dB which is comparable to or better than other SML results [16, 17]. Note that the amplitude of the third harmonic peak is underestimated because of the limit of the photodetector bandwidth.

A commercial autocorrelator (APE pulse check, Angewandte Physik & Elektronik GmbH) was used to measure the characteristics of laser pulses. Figure 5a shows the experimental result of the second-order autocorrelation trace for the Stokes wave at the maximum output power. It can be

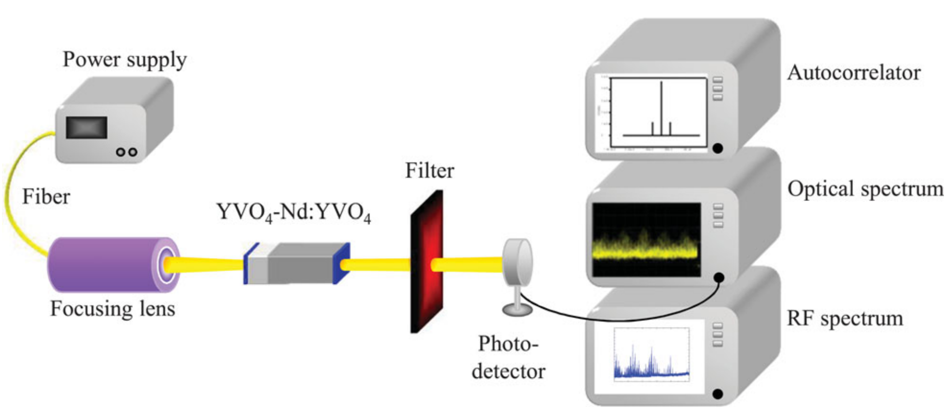

Figure 2 Experimental setup for the monolithic laser cavity with self-mode locking and stimulated Raman scattering concurrently.

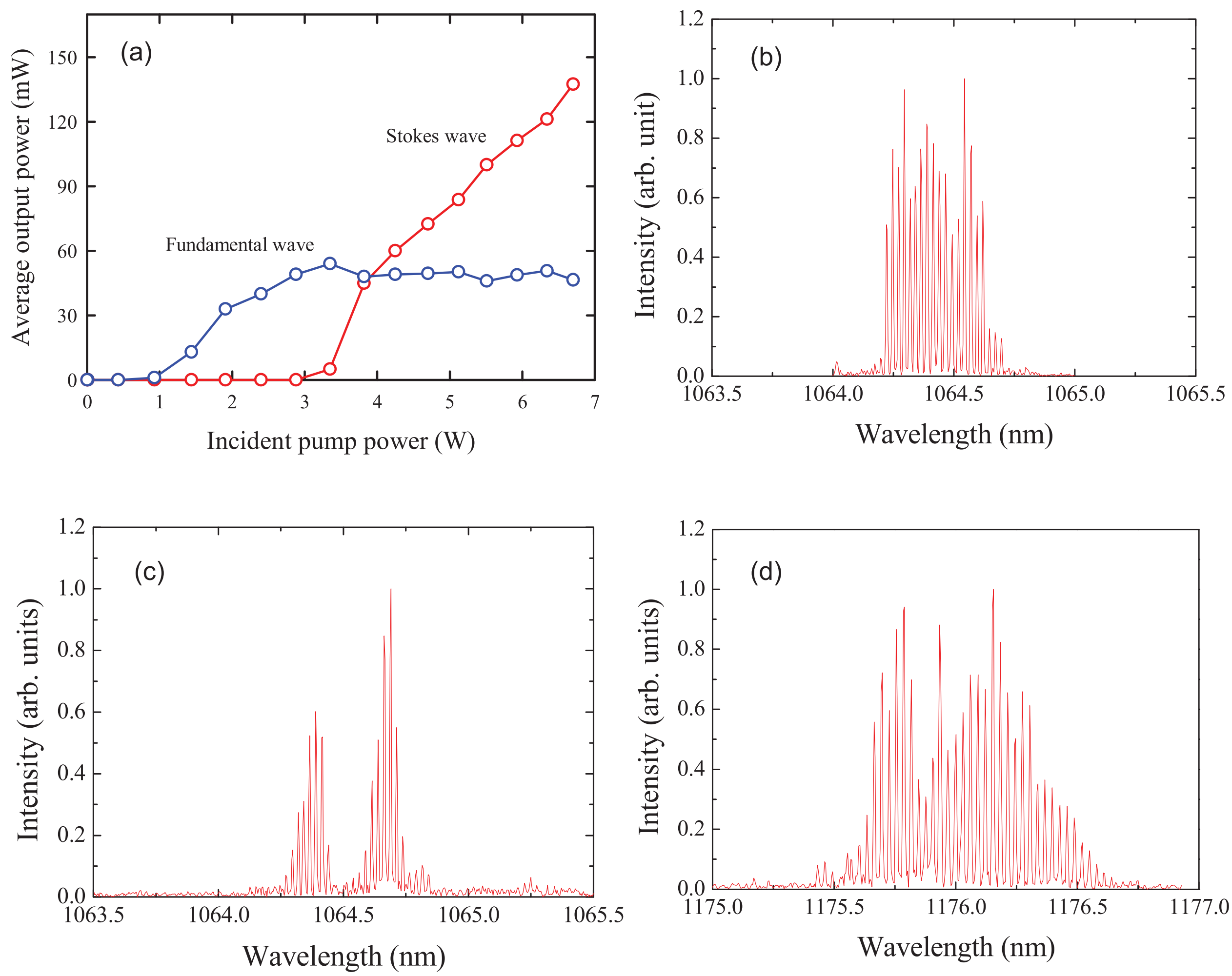

Figure 3 (a) Average output power versus the incident pump power for the monolithic self-Raman laser. (b) Optical spectrum for the fundamental wave at a pump power of 3.2 W (just below the SRS threshold). (c) Optical spectrum for the fundamental wave at a pump power of 6.5 W (far above the SRS threshold). (d) Optical spectrum for the Stokes wave at a pump power of 6.5 W.

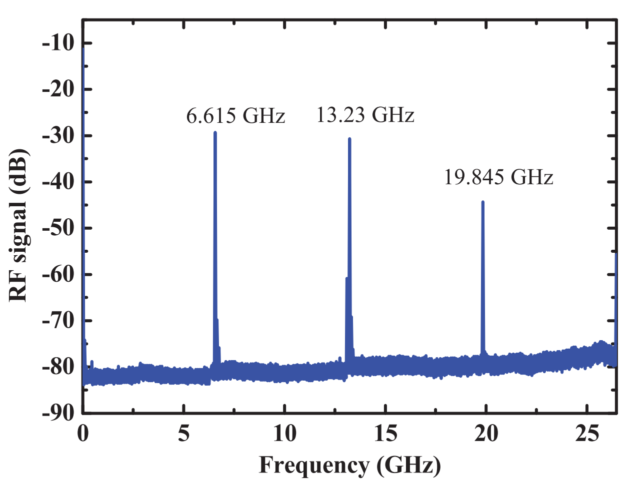

Figure 4 Experimental RF spectrum for the Stokes wave with a span of 26.5 GHz and a resolution bandwidth of 100 kHz.

seen that the second-order autocorrelation trace displays a pulse train with a period of 150 ps. The nearly perfect pulse train implies the mode-locked operation to be significantly stable. The experimental result for the single pulse of the second-order autocorrelation trace is shown in Fig. 5b. Assuming the sech^2-shaped temporal profile, the pulse duration was estimated to be 2.9 ps. From Fig. 3d, the full width at half-maximum (FWHM) of the lasing spectrum for the Stokes wave can be found to be approximately 0.42 nm. With the measured data, the time–bandwidth product of the mode-locked pulse can be calculated to be 0.34, which is quite close to the Fourier-limited value of 0.32.

4. Conclusion

In summary, we have experimentally fulfilled the generation of a Raman frequency comb from a monolithic crystal laser with the combined process of SML and SRS. At a

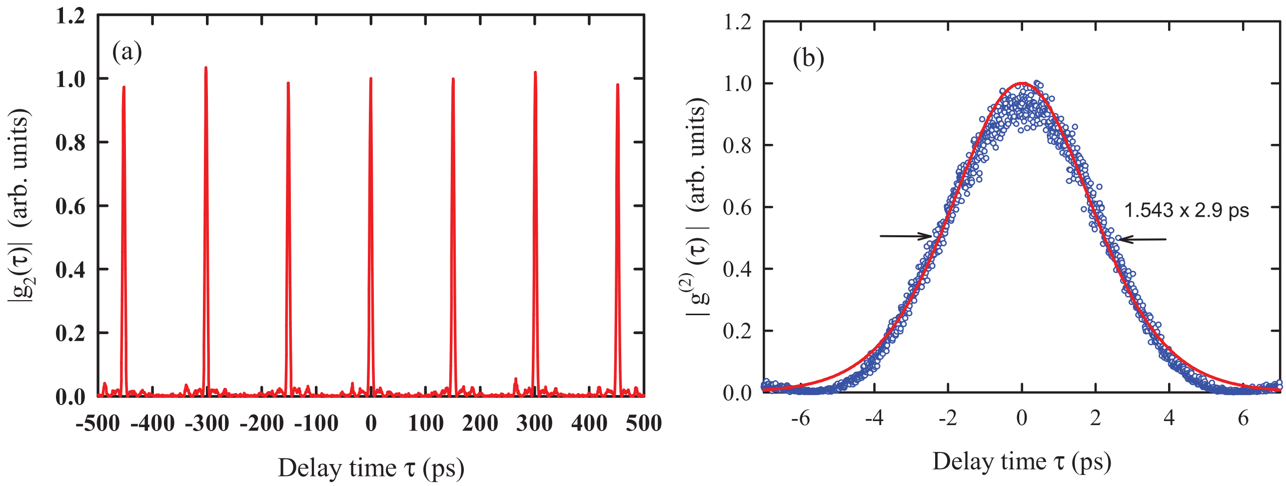

Figure 5 (a) Experimental result of the second-order autocorrelation trace for the Stokes wave at the maximum output power. (b) Experimental result for the single pulse of the second-order autocorrelation trace.

pump power of 6.5 W, we obtained an output power of 140 mW for the Stokes wave with a pulse width as narrow as 2.9 ps at a pulse repetition rate of 6.615 GHz. We have observed that below the SRS threshold the frequency comb could be formed in the fundamental wave with the SML process. Above the SRS threshold, the monolithic SML laser was found to emit the Stokes wave with a Raman frequency comb that was effectively expanded by the width of the Raman gain. It is believed that the present discovery can provide a novel method for generating mode-locked self-Raman lasers and useful insights into the monolithic intracavity SRS process.

Acknowledgements. The authors acknowledge the National Science Council of Taiwan for their financial support of this research under contract NSC 100–2628-M-009 -001 -MY3.

Received: 15 January 2014, **Revised:** 4 March 2014, **Accepted:** 14 April 2014

Published online: 16 May 2014

Key words: stimulated Raman scattering, monolithic cavity, self mode locking, frequency comb.

References

[1] J. L. Hall and T. W. Hänsch, History of optical comb development, in Femtosecond Optical Frequency Comb, J. Ye and S.T. Cundiff, Eds. (Springer, New York, NY, 2004).
[2] R. K. Shelton, L.-S. Ma, H. C. Kapteyn, M. M. Murnane, J. L. Hall, and J. Ye, Science **293**, 1286–1289 (2001).
[3] J. C. Diels and W. Rudolph, Ultrashort Laser Pulse Phenomena: Fundamentals, Techniques, and Applications on a Femtosecond Time Scale (Elsevier Inc., Burlington, VT, 2006).
[4] S. T. Cundiff and J. Ye, Rev. Mod. Phys. **75**, 325 (2003).
[5] T. J. Kippenberg, R. Holzwarth, and S. A. Diddams, Science **339**, 555–559 (2011).
[6] T. Herr, K. Hartinger, J. Riemensberger, C. Y. Wang, E. Gavartin, R. Holzwarth, M. L. Gorodetsky, and T. J. Kippenberg, Nature Photon. **6**, 480–487 (2012).
[7] J. S. Levy, A. Gondarenko, M. A. Foster, A. C. Turner-Foster, A. L. Gaeta, and M. Lipson, Nature Photon. **4**, 37–40 (2010).
[8] A. B. Matsko, A. A. Savchenkov, W. Liang, V. S. Ilchenko, D. Seidel, and L. Maleki, Opt. Lett. **36**, 2845–2847 (2011).
[9] H. A. Haus, J. Sel. Top. Quantum Electron. **6**, 1173–1185 (2000).
[10] S. Pekarek, T. Südmeyer, S. Lecomte, S. Kundermann, J. M. Dudley, and U. Keller, Opt. Exp. **19**, 16491–16497 (2011).
[11] P. Klopp, U. Griebner, M. Zorn, and M. Weyers, Appl. Phys. Lett. **98**, 071103 (2011).
[12] M. Hoffmann, O. D. Sieber, V. J. Wittwer, I. L. Krestnikov, D. A. Livshits, Y. Barbarin, T. Südmeyer, and U. Keller, Opt. Exp. **19**, 8108–8116 (2011).
[13] H. Liu, J. Nees, and G. Mourou, Opt. Lett. **26**, 1723–1725 (2001).
[14] W. Z. Zhuang, M. T. Chang, H. C. Liang, and Y. F. Chen, Opt. Lett. **38**, 2596–2599 (2013).
[15] A. A. Lagatsky, A. R. Sarmani, C. T. A. Brown, W. Sibbett, V. E. Kisel, A. G. Selivanov, I. A. Denisov, A. E. Troshin, K. V. Yumashev, N. V. Kuleshov, V. N. Matrosov, T. A. Matrosova, and M. I. Kupchenko, Opt. Lett. **30**, 3234–3236 (2005).
[16] G. Q. Xie, D. Y. Tang, L. M. Zhao, L. J. Qian, and K. Ueda, Opt. Lett. **32**, 2741–2743 (2007).
[17] S. Uemura and K. Torizuka, Appl. Phys. Exp. **1**, 012007 (2008).
[18] H. C. Liang, R. C. C. Chen, Y. J. Huang, K. W. Su, and Y. F. Chen, Opt. Exp. **16**, 21149–21154 (2008).
[19] H. C. Liang, Y. J. Huang, W. C. Huang, K. W. Su, and Y. F. Chen, Opt. Lett. **35**, 4–6 (2010).
[20] H. C. Liang, Y. J. Huang, Y. C. Lin, T. H. Lu, Y. F. Chen, and K. F. Huang, Opt. Lett. **34**, 3842–3844 (2009).
[21] Y. F. Chen, Opt. Lett. **29**, 2632–2634 (2004).

[22] Y. F. Chen, Opt. Lett. **29**, 1915–1917 (2004).
[23] H. Y. Zhu, Y. M. Duan, G. Zhang, C. H. Huang, Y. Wei, W. D. Chen, L. X. Huang, and Y. D. Huang, Appl. Phys. B **103**, 559–562 (2011).
[24] V. N. Burakevich, V. A. Lisinetskii, A. S. Grabtchikov, A. A. Demidovich, V. A. Orlovich, and V. N. Matrosov, Appl. Phys. B **86**, 511–514 (2007).
[25] A. J. Lee, H. M. Pask, D. J. Spence, and J. A. Piper, Opt. Lett. **35**, 682–684 (2010).
[26] W. Liang, V. S. Ilchenko, A. A. Savchenkov, A. B. Matsko, D. Seidel, and L. Maleki, Phys. Rev. Lett. **105**, 143903 (2010).
[27] D. J. Spence, P. Dekker, and H. M. Pask, IEEE J. Sel. Top. Quantum Electron. **13**(3), 756–763 (2007).